Catalysis Today 149 (2010) 40–46

Contents lists available at ScienceDirect

Catalysis Today

journal homepage: www.elsevier.com/locate/cattod

Middle distillates from hydrocracking of FT waxes: Composition, characteristics and emission properties

Vincenzo Calemma *, Chiara Gambaro, Wallace O. Parker Jr., Rosa Carbone, Roberto Giardino, Pietro Scorletti

Eni R&M, Via Maritano 26, 20097 San Donato Milanese, MI, Italy

ARTICLE INFO

Article history:
Available online 21 April 2009

Keywords:
Fischer–Tropsch
Wax
Hydrocracking
Emission
Hydroisomerization

ABSTRACT

A light cobalt catalyzed Fischer–Tropsch (FT) wax was subjected to hydrocracking in the range of temperature 319–351 °C and hydrogen pressure between 3.5 and 6.0 MPa. The catalyst used was platinum on amorphous silica–alumina. Hydrocracking reaction led to an increase of middle distillate yield up to 85% with a contemporary increase of iso-paraffins concentration which resulted in a remarkable improvement of cold flow properties of the products. The freezing point of C_{10}–C_{14} fraction passed from −23 to −45 °C while the pour point of C_{15}–C_{22} fraction decreased from 13 to −23 °C. The latter fraction displayed high cetane numbers ranging between 75 and 80. Changes in carbon distribution and molecular structure of products during hydrocracking have been rationalized in the light of the accepted hydrocracking mechanism where *n*-paraffins undergo to consecutive isomerization reactions leading to isomers with progressively higher branching degree and concomitant cracking reaction. Experimental evidences support the view that apparent reactivity of *n*-paraffins is chain length dependent, increasing with the molecular weight. Detailed characterization by NMR and GC showed that branching groups abundance in the middle distillate products was the following: methyl ≫ ethyl > propyl.

Emission tests carried out with FT diesel and commercial ultra low sulfur diesel showed that FT diesel has excellent combustion properties and leads to a reduction of emissions.

1. Introduction

In the last decades the depletion of oil reservoirs, along with a higher attention towards environmental problems, has stimulated an increasing interest towards the conversion of natural gas to liquid fuels [1]. The gas-to-liquids technology via low temperature Fischer–Tropsch (FT) synthesis is basically the conversion of synthesis gas into a mixture of liquid hydrocarbons, mainly normal paraffins (>90%) and small amount of olefins and alcohols. The FT product distribution is well described by the Anderson–Schulz–Flory (ASF) model [2], based on a chain growth mechanism involving successive additions of a monomer to the absorbed chain precursor. Accordingly, the hydrocarbons concentration decreases with chain length [3]. As a consequence of this continuous distribution and the need to lower as much as possible gas selectivity, a large fraction of the FT products have boiling point higher than 350 °C. Yields in the middle distillate range are rather limited especially with the current cobalt catalyzed, low temperature slurry FT technologies, where the distribution is strongly shifted towards long chain paraffins. Moreover, as a consequence of their paraffinic nature FT derived middle distillates display high cetane numbers (>75) but very poor cold properties. This poses problems both for their direct use and even as a blending component for diesel pool.[1] In spite of the efforts, the improvement of the intrinsic selectivity of the FT synthesis towards desired fractions (i.e. middle distillates) has met with limited success. Different options have been proposed for the post treatment of FT waxes [4–6] but it is generally accepted that the most effective route to maximize the overall middle distillate yield is to subject the FT wax to a hydrocracking step [7–9]. During hydroconversion two main reactions occur: hydroisomerization and hydrocracking of aliphatic chains. The first reaction route leads to a marked improvement of cold flow properties while the latter is responsible for the increase of middle distillate yields. When the reaction is carried out in suitable operating conditions and using a proper

* Corresponding author. Tel.: +39 02 520 46367.
E-mail address: vincenzo.calemma@eni.it (V. Calemma).

[1] The CFPP (cold filter plug point) of a FT gas oil (250–370 °C) is 23 °C.

0920-5861/$ – see front matter © 2009 Elsevier B.V. All rights reserved.
doi:10.1016/j.cattod.2009.03.018

catalyst the cold flow properties can be remarkably enhanced while the middle distillate yields range between 80% and 85% [10]. This solution has been extensively analyzed, as widely reported in literature [11–14].

In the last two decades environmental factors have progressively led to the promulgation of more stringent automotive emission standards. The European Union has established emission standards to set limits for vehicles exhaust gasses, in terms of NOx, CO, HC and particulate emissions [15] and these are regularly updated. The current fuel regulations require a minimum diesel cetane number of 51 and a maximum sulfur content for gasoline and diesel of 50 ppm (2005), while "sulfur free" fuels ($\leq$10 ppm) must be available since 2009 [16]. FT derived middle distillates are characterized by the absence of sulfur and aromatic compounds whose presence in petroleum derived fuels invariably leads to higher pollutant emissions. Several studies aimed at investigating the effect of diesel composition indicate that using FT derived diesel fuel neat or as a blending component leads to a marked reduction in exhaust emissions [17,18].

The present study describes the hydrocracking of FT wax to middle distillate using a noble metal on SiO_2-Al_2O_3 catalyst. Overall middle distillate yields, changes in products distribution and modifications of the molecular structure at increasing hydrocracking severity have been investigated. Furthermore, the emissions of FT diesel and commercial ultra low sulfur diesel were determined.

2. Experimental

Hydrocracking tests were carried out in a bench scale trickle bed reactor operated in down flow mode (height of the catalyst bed: 100 mm; internal diameter: 16 mm). The reactor was charged with 9 g of platinum supported on amorphous SiO_2-Al_2O_3 catalyst, previously crushed and sieved (average particle size: 0.625 mm). The catalyst pellet diameter was reduced in order to approximate plug flow behavior, minimizing back mixing and wall effect, according to empirical correlations reported in literature [19].

The feed used throughout the experiments was a light paraffinic FT wax, characterized by a C_{22+} weight fraction of about 36%.

The range of operating conditions was: temperature 319–351 °C, pressure 3.5–6.0 MPa, H_2/wax ratio 0.06–0.15 kg/kg and space velocity (WHSV) 1–3 h^{-1}. Liquid products analysis was carried out with a GC HP-5890 II equipped with on column injection system, electronic pressure control, and FID detector. The column used was a SPB-1 (Supelco) 15 m (l) $\times$ 0.53 mm (i.d.) $\times$ 0.1 μm (film thickness). Temperature programming of the oven was 1 min at 0 °C then up to 315 °C, with a linear ramp rate of 5 °C min^{-1} and a holding time at the final temperature of 37 min.

Temperature programming of injector was 1 min at 50 °C then up to 330 °C with a linear ramp rate of 5 °C min^{-1} and a holding time at the final temperature of 37 min.

Upon integration of the GC trace, it is possible to obtain the liquid phase composition as weight percentage of normal and iso-paraffin lump of each single aliphatic chain present. Gaseous fraction of products was analyzed by a GC HP 5890 II equipped with a FID detector and automatic sampling loop. The column used was a HP PONA crosslinked methyl siloxane, 50 m (l) $\times$ 0.2 mm (i.d.) $\times$ 0.5 μm (film thickness). Temperature programming of the oven was 7.5 min at 35 °C then up to 70 °C with a linear ramp rate of 3 °C min^{-1}, subsequently up to 220 °C at 7.5 °C min^{-1} and keeping the final temperature for 45 min.

For both analyses the carrier used was helium.

The overall composition of hydrocracking products was obtained by merging together the results of liquid and gas products analyses according to their weight fraction. The method above reported allowed to obtain the concentration of each single *n*-paraffin and the respective iso-paraffin lump.

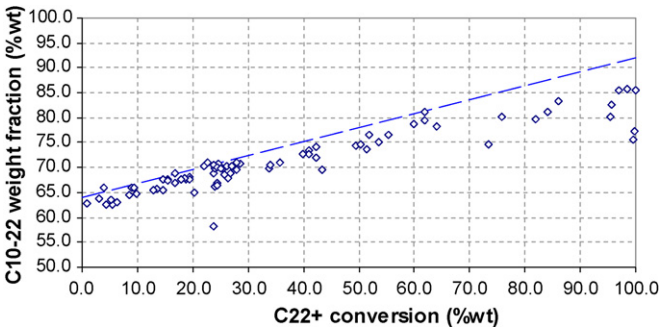

Fig. 1. Middle distillate yield vs. C_{22+} fraction conversion. Symbols refer to experimental results; the dashed line refers to the theoretical yields.

A second method, reported here below, characterized by a higher resolution of the lighter components allowed to distinguish among the different classes of isomers such as mono-, di- and tri-branched paraffins for chain lengths lower than 25 carbon atoms.

In this case the liquid products were analyzed with a GC HP 6890 Plus T equipped with electronic pressure control, FID detector and supplied with a switching system (G2855B Deans Switching System) which allowed to send to the column used for the separation, the fraction C_{30-} of the liquid sample while the heavier fraction is vent out. The column was a HP-5 high speed 5% phenyl methyl siloxane, 50 m (l) $\times$ 0.2 mm (i.d.) $\times$ 0.5 μm (film thickness).

Temperature programming of the oven was 3 min at 35 °C then up to 180 °C, with a linear ramp rate of 2 °C min^{-1}, keep 180 °C for 75 min then to 220 °C at 1.5 °C min^{-1}, keep 220 °C for 102 min then to 250 °C at 1.2 °C min^{-1}. Finally keep 250 °C for 71 min.

Identification of GC peaks was accomplished by GC–MS analysis and when possible by addition of pure compounds to the mixture of products.

An in depth characterization of branching in the diesel fraction was also carried out by ^{13}C NMR technique (described later).

The chemical–physical properties of kerosene and diesel fuel produced from FT wax were determined by standard methods.

3. Results and discussion

3.1. Products selectivity

As shown in Fig. 1, middle distillate (C_{10}–C_{22}) yield increases up to 80–85 wt% along with C_{22+} fraction conversion. Only at conversion values higher than 60% it is possible to observe the reduction of the curve slope, indicating an increase of consecutive hydrocracking reactions leading to lighter products formation. It is worth noticing that even at the highest level of conversion the presence of consecutive reaction is rather limited so allowing to carry out the reaction at high conversions without lowering too much the middle distillate selectivity.[2]

In the evaluated case, the selectivity to naphtha (i.e. C_5–C_9) is rather low while the production of gas (C_1–C_4 compounds) is negligible. Gas and naphtha fractions reach maximum yields of 3–5 wt% and 10–13 wt%, respectively.

The low production of C_1–C_4 compounds, the high selectivity values for middle distillates and the constancy of the kerosene (C_{10}–C_{14})/diesel (C_{15}–C_{22}) ratio, shown in Fig. 2, are consistent with a mechanism where the consecutive reactions of the first

[2] Dispersion of data in Fig. 1 is mainly caused by the different operating conditions which affect the selectivity in the C_{10}–C_{22} fraction.

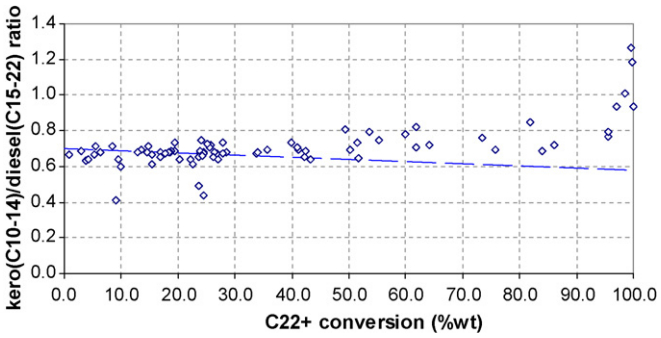

Fig. 2. Kerosene (C_{10}–C_{14})/diesel (C_{15}–C_{22}) ratio vs. C_{22+} fraction conversion. Symbols refer to experimental results; the dashed line refers to the theoretical kerosene/diesel ratio.

formed products are limited and hydrocracking of each normal paraffin occurs according to an "ideal hydrocracking", where the scission probability of the C–C bonds of the aliphatic chains is the same with the exception of the two terminal C–C bonds [10,20]. As a matter of fact, as shown in Fig. 2, a pure ideal behavior would lead to a decrease of the (C_{10}–C_{14})/(C_{15}–C_{22}); however the experimental data are rather close to the theoretical data. The latter, worked out assuming that the fraction C_{22-} does not undergo to cracking reaction and an equimolar distribution of products resulting from the cracking of the C_{22+} *n*-paraffins, except those resulting from the breakage of C–C bonds in α and β position to the terminal carbon of aliphatic chain, which are supposed to be zero. Furthermore, the very low yields of methane and ethane even at high conversion values indicate that alkanes reaction via hydrogenolysis is scarce and the conversion of normal paraffins occurs almost exclusively via carbeniun chemistry.

The comparison of carbon distribution in the feed and in the products obtained at different conversion degrees, shown in Fig. 3, points out the progressive decrease of heavier components and the contemporary increase of compounds in middle distillate range.

Literature data show that the reactivity of *n*-alkanes increases with the molecular weight [21]. This can be accounted for by the fact that the reactivity is expected to be proportional to the number of secondary carbon atoms per molecule or, as proposed by Sie, to C_{n-6} and C_{n-4} for hydrocracking and hydroisomerization, respectively [22]. However, as reported in several works [23,24], the higher reactivity of heavier *n*-paraffins can be also ascribed to their stronger physisorption, which cause an enrichment of the heavier components on the catalyst surface respect to the bulk composition and consequently to higher reaction rates. Denayer et al. [25] reported the hydroconversion of a quaternary mixture of *n*-paraffins C_6–C_9 in vapor phase conditions. It was observed that

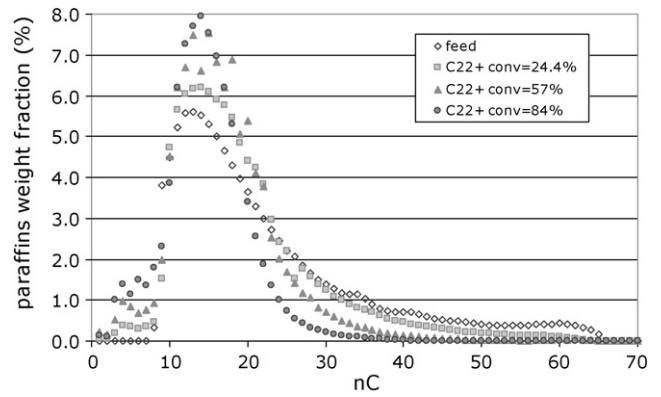

Fig. 3. Products yields distribution obtained at different C_{22+} fraction conversion.

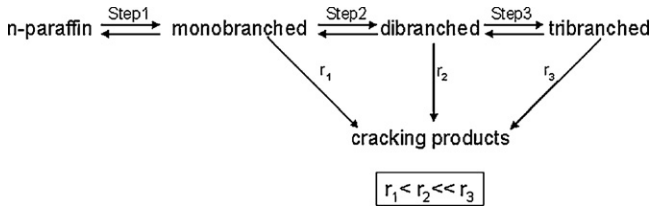

Fig. 4. Normal paraffin hydrocracking reaction mechanism. Iso-paraffins and cracking products formation.

longer alkanes were preferentially converted due to the competitive adsorption favoring the heavy compounds.

With bifunctional catalysts having a good balance between acid and hydro-dehydrogenating functions, conversion of *n*-alkanes occurs through a series of consecutive reactions, where the *n*-alkanes are first isomerized into mono-branched isomers which undergo subsequent isomerization steps and cracking reaction, as shown in a simplified manner in Fig. 4 [26].

Distributions of normal and iso-paraffins at different levels of conversion, shown in Fig. 5, are consistent with the accepted reaction pathway and the higher isomer content of heavier aliphatic chains would merely reflect the increasing conversion degree of the single *n*-paraffin due to their higher reactivity in comparison with the lighter ones. However, the apparent overall reactivity of normal paraffin could be the result of different factors such as intrinsic reactivity, physisorption and vapour–liquid equilibrium (VLE) in the reaction environment. In this regard, it has been recently shown that, in hydroconversion of a binary mixture of *n*-heptane and *n*-nonane, the physisorption behaviors in liquid phase is very different from that observed in vapor phase [27,28]. More specifically, both in liquid and vapor phase, the *n*-nonane is more reactive than *n*-heptane but the difference in reactivity is much more pronounced in vapor phase than in liquid phase. On the basis of the results obtained the authors concluded

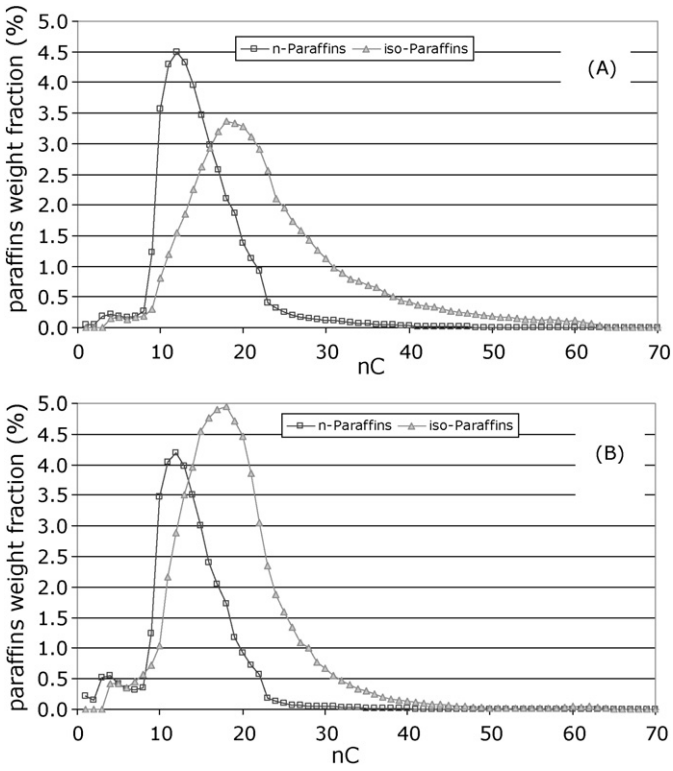

Fig. 5. Normal and iso-paraffins yields distribution at different C_{22+} fraction conversions. (A = 24.3% conversion; B = 57.0% conversion).

that the observed rates in liquid phase conditions mainly reflects the intrinsic reactivity of normal paraffins rather than differences of the physisorption behavior. In our case the observed increase of reactivity of the heavier alkanes could be only partially the result of stronger physisorption or intrinsic reactivity, and a significant role could be played by the VLE as well. Actually, it is known that VLE in the range of operating condition used in this work leads to a liquid phase enriched in the heavier components [29].

3.2. Products isomerization

One of the major drawbacks of middle distillates derived from FT synthesis is strictly connected with their paraffinic nature which gives very poor cold flow properties. The isomerization reaction plays a fundamental role in FT wax upgrading because it allows a lowering of the melting point of paraffinic compounds with a consequent improvement of the cold flow properties of the produced middle distillates. The data in Fig. 6 show, both for kerosene and diesel fractions, a sharp increase of the isomer content at the lower bound of conversion followed by a slower increase up to values of ~0.6 for kerosene and ~0.85 for diesel.

To achieve a reliable esteem of the cold flow properties of middle distillates it is not enough to determine iso-paraffins content but it is necessary to get a detailed characterization of the isomer fraction. Although, from a qualitative stand point, a direct relationship between isomer content and melting point is expected, the extent of the decrease significantly depends on the degree, the position and the length of the branching. Branching positions in the middle of the chain have a higher effect than those near the end of the chain, while longer side chains lead to a higher decrease of melting point [30]. The results reported in Fig. 7, show that both mono- and multi-branched isomers concentrations in the C_{22-} fraction increase with conversion. At lower conversion level the concentration of mono-branched isomers is higher than multi-branched but the difference decreases at higher conversion up to observe an inversion of concentrations at the highest bond values. The branching evolution can be readily interpreted in terms of the above discussed *n*-paraffins conversion pathway, where mono-branched isomers are the first formed products and the formation of isomers with higher branching degree occurs by consecutive reactions [26,31].

A more detailed analysis reveals that mono-branched isomers lump is a mixture of methyl-paraffins, with lower amounts of ethyl-paraffins and traces of propyl-paraffins. Results reported in Fig. 8 display that monomethyl-paraffins are, by far, the most abundant isomers and the methyl/ethyl/propyl-isomers ratio up to

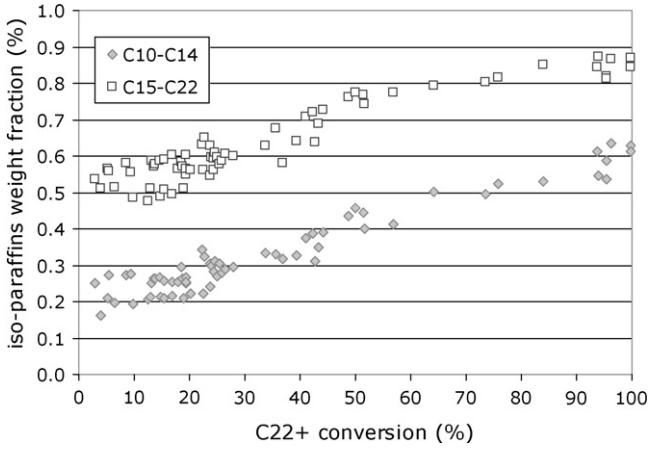

Fig. 6. . Iso-paraffins yields for kerosene (C_{10}–C_{14}) and diesel (C_{15}–C_{22}) fractions vs. C_{22+} fraction conversion.

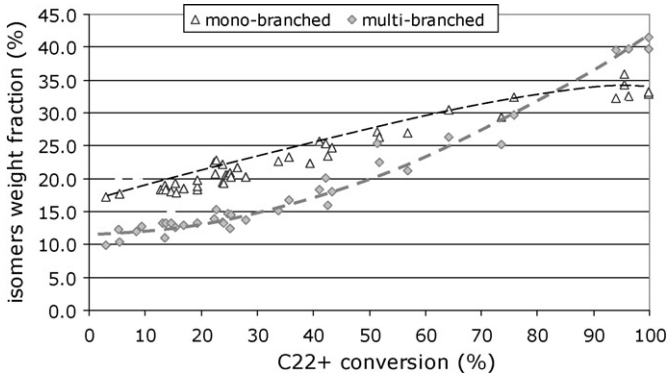

Fig. 7. Mono- and multi-branched isomers yield in the C_{22-} fraction vs. C_{22+} fraction conversion.

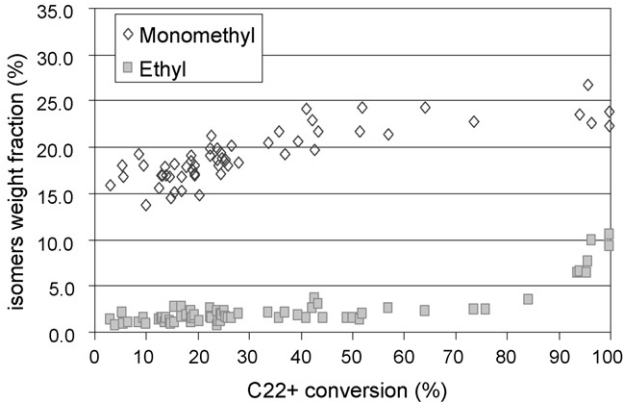

Fig. 8. Monomethyl and ethyl-isomers yield in the C_{22-} fraction vs. C_{22+} fraction conversion.

50% C_{22+} fraction conversion is approximately 100/10/1. Furthermore, mono-methyl isomers concentration increases with conversion up to about 60% and remains constant thereof, while ethyl-isomers weight fraction shows a slightly increase up to 90% conversion followed by a more rapid increase for higher values.

Formation of methyl branching can be explained according to protonated cyclopropane mechanism (PCP) [32], while the formation of ethyl and propyl isomers, by analogy with the PCP mechanism, may result by the formation of protonated cyclobutanes and protonated cyclopentanes as intermediate stage, respectively. With increasing the number of carbon atoms of the protonated rings their formation probability rapidly decreases and, consequently, the formation of branching longer than methyl group [33]. Alternatively, as proposed by Weitkamp [34], ethyl and propyl branching may result from consecutive isomerization reaction of methyl isomers via classical isomerization of type A, as depicted in Fig. 9.

A clear distinction between the two routes is not possible presently. However, we notice that the increase of ethyl branching concentration at the higher bond of conversion where high methyl

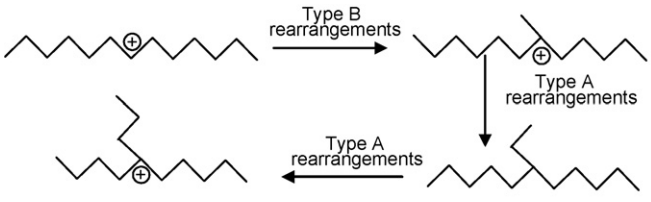

Fig. 9. . Route for ethyl and propyl branching formation [35].

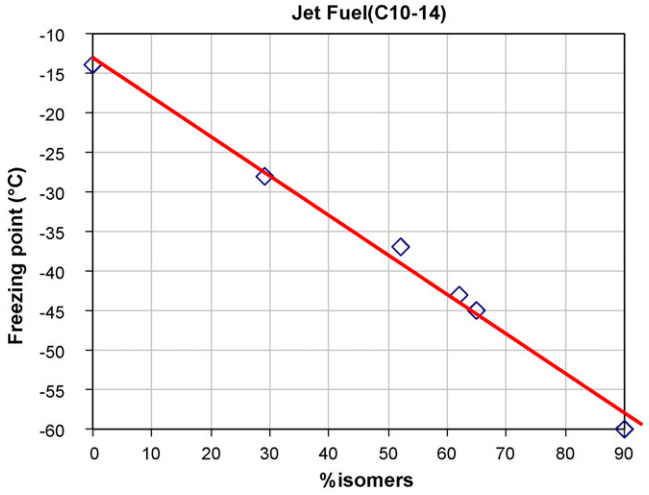

Fig. 10. Relationship between isomer content and Freezing Point in FT kerosene (C_{10}–C_{14} fraction).

branching is already present supports the view that ethyl branching may be formed via classical type A rearrangement rather than via protonated cyclobutane.

3.3. Products quality

As reported before, the iso-paraffins content of kerosene and diesel fractions increase with C_{22+} conversion. Depending on operating conditions and conversion degree, the isomer content of kerosene and diesel fraction in the tests ranges between 20–65% and 40–85%, respectively. As a consequence, the freezing point (FP) of kerosene ranges between −20 and −49 °C while the pour point (PP) of diesel is between 13 and −23 °C. Besides the isomer content the cold flow properties also depend on distillation curve and lower FP and PP can be easily obtained slightly lowering the final boiling point of the fraction. Rough correlations of FP and PP with isomers content in kerosene and diesel fraction are reported in Figs. 10 and 11, respectively.

Similarly to the cold flow properties, also cetane number – a measure of the autoignition tendency of a diesel fuel – strictly depends on chain length and branching degree of paraffin. Iso-paraffins have lower cetane numbers compared with linear paraffins. Higher branching degrees and longer alkyl bearing groups result in a lower cetane number [35,36]. As reported in Fig. 12, the cetane number of C_{15}–C_{22} fraction decreases along with

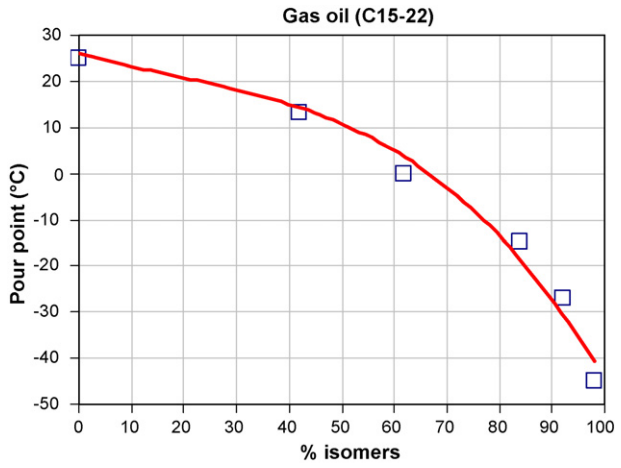

Fig. 11. Relationship between isomer content and pour point in FT diesel (C_{15}–C_{22} fraction).

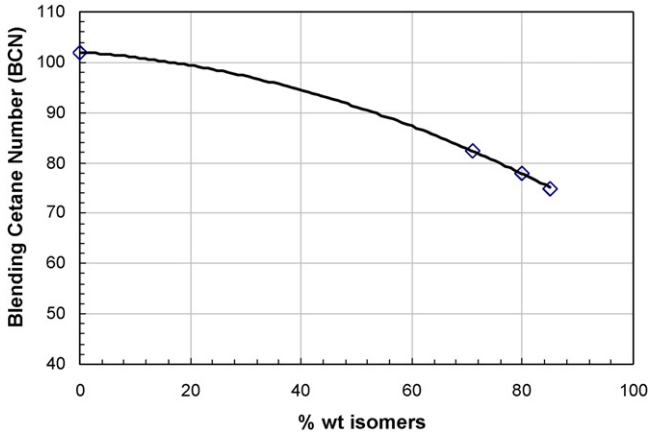

Fig. 12. Blending cetane number as a function of isomers content in FT diesel (C_{15-22} fraction).

the increase of isomer content. However, it is worth noticing that even at high isomer concentration the cetane number is still remarkably high. The reason for this is due to the fact that the large part of branching is of methyl type while the degree of branching is relatively low. The Cetane numbers for iso-paraffin fraction, calculated on the basis of the known cetane numbers for *n*-paraffins and chain length distribution of *n*- and iso-paraffins lumps, range between 75 and 70. The reported value at zero isomer content has been calculated on the basis of cetane numbers available in literature and chain length distribution.

In the light of the obtained results, the behavior of a middle distillate obtained on larger scale from FT wax has been evaluated. In the present case the wider distillation curve is more representative of a commercial diesel cut (C_{11}–C_{21} fraction). The product was characterized by ^{13}C NMR and detailed GC method. Due to inherent uncertainties and complexities involved with analyzing complete ^{13}C NMR spectra, a simple strategy was adopted here. Only signals from the methyl groups were considered. These signals were clearly distinguished from those of the methylene carbons by the DEPT (distortionless enhancement by polarization transfer) NMR technique. Individual signals were assigned based on chemical shift [37] for the methyl carbons of CH_3 (19.1–19.7 ppm), C_2H_5 (10.8 ppm) and C_3H_7 (14.4 ppm) branching groups. 20% of all the carbon atoms are methyl groups. Of these, half are at the terminus of a linear segment (at least four carbons long) the remaining belongs to branching made up of methyl (80%), ethyl (10%) and propyl (8%) groups, respectively. The average branching sites per molecule is 1.54.

The results of detailed GC analysis reported in Table 1 allow us to do further remarks. Similarly to the NMR results, the most abundant branching group is the methyl group which account for the 80–85% of the overall branching groups while the ethyl and the propyl groups are present in much lower concentration. As stated before, the predominance of methyl group is in agreement with the accepted isomerization mechanism. The degree of isomerization increases with the chain length passing from 33% to 85% for C_{12}–C_{20}, respectively. Differently the relative concentration of mono-methyl paraffins shows a decrease for longer chain length with a contemporary increase of isomers with higher branching degree. Both results are in agreement with the higher reactivity of heavier paraffins and the reaction pathway for hydroisomerization of *n*-paraffins presented before according which, in first approximation, the conversion of *n*-paraffin occurs through a series of consecutive isomerization reactions. In this case the decrease of mono-methyl paraffin merely mirrors the increasing degree of advancement of the reaction as a function of chain length as witnessed by the higher degree of isomerization. The calculated average branching

Table 1
Detailed GC analysis of FT diesel. Distribution of isomer and branching types as function of chain length.

Chain length	*i*-Paraffin (wt%)	*n*-Paraffin (wt%)	*i*-Paraffin[a] (wt%)	Me[b,c] (wt%)	DMe[b,c] (wt%)	Et[b,c] (wt%)	DB+[b,c] (wt%)
C_{10}	–	0.01					
C_{11}	0.14	0.86	13.88	62.95	24.68	11.77	0.59
C_{12}	3.16	6.33	33.31	62.49	20.47	5.74	11.29
C_{13}	7.46	6.45	53.61	58.44	16.85	11.69	13.01
C_{14}	8.14	5.35	60.36	59.31	22.06	4.20	14.43
C_{15}	8.45	4.44	65.55	64.03	20.98	3.40	11.57
C_{16}	8.14	3.51	69.83	49.61	11.81	15.71	22.85
C_{17}	7.98	2.58	75.53	53.37	17.59	5.55	23.47
C_{18}	7.66	1.98	79.48	48.73	6.67	8.42	36.16
C_{19}	6.95	1.34	83.83	48.93	18.54	6.00	26.52
C_{20}	5.86	1.00	85.45	39.10	17.64	7.61	35.64
C_{21}	2.20	0.02	98.96	36.44	21.54	8.92	33.08
Total %	66.10	33.90		53.21	16.91	7.67	22.20

The values in the last line refers to the percentage of different classes of iso-paraffins on the basis of the overall content of iso-paraffins.
[a] Percentage for the given chain length.
[b] Me: methyl-paraffin; DMe: dimethyl-paraffins; Et: ethyl-paraffins; DB+: tribranched paraffins plus dibranched paraffins with alkyl groups longer than methyl and propyl-paraffins.
[c] The values are given on isomer basis.

Table 2
FT and ultra low sulfur diesel properties.

Parameter	Method	FTD	ULSD	EN 590 spec
Density at 15 °C (kg/l)	ASTM D4052	0.777	0.831	0.820–0.845
Distillation (°C)	ASTM D86			
10 vol%		240	230	
50 vol%		265	280	
90 vol%		306	341	
Flash point	ASTM D93	103	75	
Aromatics (wt%)	EN 12916			
1 Ring		<1	19.9	
2 Rings+		0	2.8	<11
Total		<1	22.7	
Kin. Viscosity at 40 °C (cSt)	ASTM D445	2.615	3.143	
Cloud point (°C)	ASTM D2500	−16	−1	
CFPP (°C)	EN 116	−18	−12	<−12
Sulfur (mg/kg)	ISO 20846	<1	4.7	<10
Cetane number	ASTM D613	80.8	55.1	>51
Lubricity	CEC-F-06-2003	600	–	<450

site per molecule is 1.52, very similar to the value calculated on the basis of NMR data.

The chemical–physical properties of the produced FT diesel (FTD) are reported in Table 2 together with a commercial ultra low sulfur diesel (ULSD) properties and diesel EN590 main specifications.

Being almost exclusively made up of normal and iso-paraffins FTD shows rather low density and extremely high cetane number, compared to commercial diesel. Aromatics and sulfur, the main responsible for the lubricity of the petroleum derived feedstock are below the detection limits [38]. Oxygenated compounds which are side products of FT synthesis could at least partially restore the poor lubricity [39,40] but they are fully hydrogenated during the hydrocracking stage. However, the lubricity of FTD can be improved to acceptable levels by using additives [41].

3.4. Emission tests

Exhaust emissions of FTD have been compared with the emissions of the commercial ULSD. The emission test investigation was carried out according to the New European driving cycle (NEDC) consisting of four repeated ECE-15 driving cycles and an Extra-Urban driving cycle (EUDC) [16]. Engine tests were performed on a light duty diesel vehicle with a common rail injection system (FIAT Stilo 1.9 JTD).

Table 3
Regulated emissions in NEDC mode (g/km).

Fuel	HC	CO	CO_2	NOx	HC + NOx	PM	l/100 km (93/116/CE)
ULSD	0.059	0.439	151.55	0.475	0.534	0.037	5.780
FTD	0.016	0.101	145.81	0.464	0.480	0.026	5.928

The results of regulated emissions are reported in Table 3. Each figure is the average of three repetitions.

The FTD caused negligible change in NOx emission, but showed more than 70% of the decrease in CO and HC emissions compared to ULSD. An improvement in terms of CO_2 of roughly 4% was obtained. Although the CO_2 levels have been lowered, the car fuel consumption was increased by roughly 3% due to the lower density of FTD.

It has been shown that the soot formation tendency heavily depends on the molecular structure [42,43]. The results indicate that the soot formation tendency decreases in the order: aromatics > naphthenes > iso-paraffins > normal paraffins. In agreement with literature results, the PM emission from the ULSD, containing aromatic and naphthenic compounds is significantly higher than those from the FTD paraffinic fuel. However, PM reduction observed with FTD is only 30% lower, not as high as expected. The reason lies in FTD very high cetane number. In fact, ignition lags vary with cetane number, thus FTD with CN = 80.8 gives ignition delays significantly shorter than ULSD having CN = 55.1. Consequently, combustion is initiated before sufficient fuel–air mixing has occurred. The weaker fuel–air mixing rate during the diffusion combustion process causes various changes in the local phenomena such as air entrainment into fuel sprays, the location of initial flame, soot clouds and/or soot precursors. All these factors can cause an increase in PM and soot formation [18]. According to this figure an increase of the isomerization degree and consequent CN reduction can lead to a further PM emissions reduction even if has been reported that, compared to *n*-paraffins, PM formation potential increases with branching and, among iso-paraffins, increases with the number of branches [44,45].

Poly aromatics hydrocarbon (PAH) emissions have been also determined. PAH are currently unregulated pollutants in automotive exhaust emissions. They may be emitted to the atmosphere associated with fine particles. Determination of individual trace level PAH in automotive exhaust emissions is complicated, not only with respect to the analysis, but also by the need to standardize sampling procedures. PAH emissions have been sampled by filter collection of the particulate. Legislative measurement of diesel

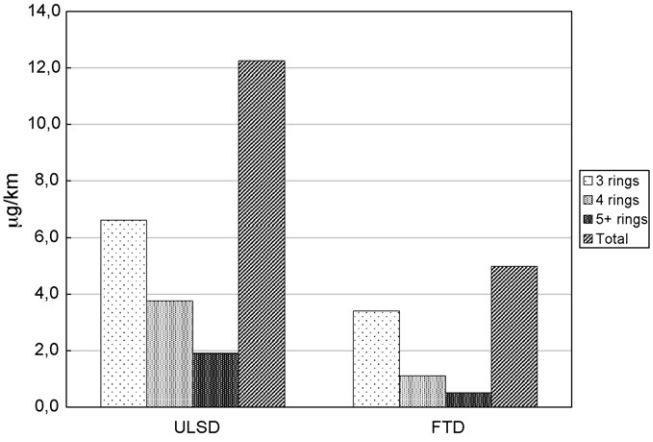

Fig. 13. Polyaromatics (3+ rings) hydrocarbon emissions.

particulate mass requires dilution tunnel sampling and Teflon (Pallflex) filter collection, from which the unregulated PAH have been extracted and analyzed. All exhaust samples filters were extracted with accelerated solvent extraction (ASE instrument) for at least 1.5 h hexane/acetone (2:1, v/v). During the extraction a mix of deuterated PAH have added to the filters as internal standard. Following extraction, a clean up routine has made to isolate the PAH from interfering compounds. The extract has been analyzed using GC with MS detector enabled to detect PAH compounds.

For PAHs emission such as benzo(*a*)anthracene, 7,12-dimethylbenzo(*a*)anthracene, benzo(*b*)fluoanthene, benzo(*k*)fluoanthene, benzo(*a*)pyrene, indeno(1,2,3-cd)pyrene and benzo(*ghi*)perylene, about 60% of the total amounts of the all PAHs emission were reduced by FTD compared with the commercial ULSD. In particular, 4 and 5+ rings PAHs were reduced by 80% (Fig. 13).

4. Conclusions

The hydrocracking behavior of a C_{10}–C_{70} FT derived wax was investigated: experimental results show that during hydrocracking longer aliphatic chains are hydrocracked preferentially leading to an increase of middle distillate cut. Furthermore, the conversion was also characterized by a low naphtha selectivity and scarce formation of C_1–C_4 fraction. The latter data together with the evolution of kerosene/diesel ratio indicate an "ideal hydrocracking" mechanism, where consecutive reactions of the primary products are negligible. The isomer content of reaction products shows a strong increase with conversion reaching values of 80% and 60% for the C_{15}–C_{22} and C_{10}–C_{14} fractions, respectively. A detailed analysis of the C_{22-} fraction in the product mixture evidenced that isomers are mainly made up of mono-branched paraffins, while multibranched are more abundant at the highest conversion levels; this behavior is consistent with the accepted hydroconversion pathway of *n*-paraffins.

FT diesel is a mixture of iso- and *n*-paraffin whose relative concentration depends largely on the operating conditions and type of catalyst used. As a consequence of the chemical nature of the components, FT diesel show a low density, due to the lack of aromatics and naphthenes, and for the same reason the cetane numbers are generally extremely high even when the isomers concentration is high. The absence of aromatics and sulfur positively affect the emission behavior but have a negative impact on lubricity which is generally well below the accepted standards. The absence of etheroatoms, aromatics and naphthenes make this fuel, from a compositional stand point, ideal for the environmental impact reduction. Results of the engine tests show that FTD lead to significant reduction of CO, HC, PM and PAHs emissions in comparison with petroleum derived diesel.

References

[1] M.E. Dry, Catal. Today 71 (2002) 227.
[2] R.A. Friedel, R.B. Anderson, J. Am. Chem. Soc. 72 (1950) 1212.
[3] G. van Der Laan, A.A.C.M. Beenackers, Catal. Rev. -Sci. Eng. 41 (1999) 225.
[4] X. Dupain, R.A. Krul, M. Makkee, J.A. Moulijn, Catal. Today 106 (2005) 288.
[5] L.P. Dancuart, J.F. Mayer, M.J. Tallman, J. Adams, J. Prep. Am. Chem. Soc. Div. Pet. Chem. 48 (2003) 132.
[6] A. de Klerk, Ind. Eng. Chem. Res. 46 (2007) 5516.
[7] S.T. Sie, M.M.G. Senden, H.M.W. Van Wachem, Catal. Today 8 (1991) 371.
[8] D.O. Leckel, D. Liwanga-Ehumbu, Energy Fuels 20 (2006) 2330.
[9] L.P. Dancuart, R. de Haan, A. de Klerk, in: A. Steynberg, M. Dry (Eds.), Stud. Surf. Sci. Catal., Elsevier, Amsterdam, vol. 152, 2004, p. 482 (Chapter 6).
[10] V. Calemma, S. Peratello, S. Pavoni, G. Clerici, C. Perego, in: E. Iglesia, J.J. Spivey, T.H. Fleisch (Eds.), Stud. Surf. Sci. Catal., Elsevier, Amsterdam, vol. 136, 2001, p. 307
[11] T.G. Kaufman, A. Kaldor, G.F. Stuntz, M.C. Kerby, L.L. Ansell, Catal. Today 62 (2000) 77.
[12] J.P. Collins, J.J.H.M. Font Freide, B. Nay, J. Nat. Gas Chem. 15 (2006) 1.
[13] D.J. O'Rear, US Patent 6890423B2 (2005).
[14] P. Euzen, C. Gueret, EP Patent 893724 (A1) (2003).
[15] Directive 98/69/EC of the European Parliament and of the Council of 13 October 1998.
[16] http://www.diesenet.com/standards/eu/ld.php.
[17] T.L. Alleman, R.L. Mc Cormick, SAE Paper 2003-01-0763, 2003.
[18] K. Nakakita, H. Ban, S. Takasu, Y. Hotta, K. Inagaki, W. Weissman, J.T. Farrell, SAE Paper 2003-01-1914, 2004.
[19] L.F. Ramírez, J. Escobar, E. Galván, H. Vaca, F.R. Murrieta, M.R.S. Luna, Pet. Sci. Technol. 22 (2004) 157.
[20] J. Weitkamp, E. Kole, Erdgas Petrochem. 31 (1978) 13.
[21] J. Weitkamp, in: J.W. Ward, S.A. Quader (Eds.), ACS Symposium Series, vol.20, American Chemical Society, Washington, DC, 1975, p. 1.
[22] S.T. Sie, Ind. Eng. Chem. Res. 32 (1993) 403.
[23] J.F. Denayer, G.V. Baron, P.A. Jacobs, J.A. Martens, Phys. Chem. Chem. Phys. 2 (2000) 1007.
[24] J.F. Denayer, G.V. Baron, J.A. Martens, P.A. Jacobs, Phys. Chem. B 102 (1998) 3077.
[25] J.F. Denayer, G.V. Baron, V. Souverijns, J.A. Martens, P.A. Jacobs, Ind. Eng. Chem. 36 (1997) 3242.
[26] V. Calemma, S. Peratello, C. Perego, Appl. Catal. A 190 (2000) 207.
[27] J.F.M. Denayer, B. De Jonckheere, M. Hioch, G.B. Marin, G. Vanbustele, J.A. Martens, G.V. Baron, J. Catal. 210 (2002) 445.
[28] J.F.M. Denayer, R.A. Ocakoglu, W. Huybrechts, B. De Jonckheere, P. Jacobs, S. Calero, R. Krishna, B. Smit, G.V. Baron, J.A. Martens, J. Catal. 220 (2003) 66.
[29] S. Correra, V. Calemma, L. Pellegrini, S. Bonomi, in: S. Pierucci (Ed.), Chem. Eng. Trans. 6 (2005) 849.
[30] Properties of Hydrocarbons of High Molecular Weight, Research Project 42 of the American Petroleum Institute, API 951, 1967.
[31] M. Steijns, G. Froment, P. Jacobs, J. Uytterhoeven, J. Weitkamp, Ind. Eng. Chem. Prod. Res. Dev. 20 (1981) 654.
[32] S.T. Sie, Ind. Eng. Chem. Res. 31 (1992) 1881.
[33] C. Marcilly, Catalyse acido-basique, Application au raffinage et à la pétrochimie, Editions Technip, Paris, vol. 1, 2003, p. 168 (Chapter 3).
[34] J. Weitkamp, Ind. Eng. Chem. Prod. Res. Dev. 21 (1982) 550.
[35] M.J. Murphy, J.D. Taylor, R.L. Mc Cormick, Compendium of Experimental Cetane Number Data, NREL/SR-540-36805, 2004.
[36] S.M. Heck, H.O. Pritchard, J.F. Griffiths, J. Chem. Soc., Faraday Trans. 94 (1988) 1725.
[37] B.R. Cook, P.J. Berlowitz, B.G. Silbernagel, D.A. Sysyn, US patent 6,210,559 (2001).
[38] P. Norton, K. Vertin, N.N. Clark, D.W. Lyons, M. Gautam, S. Goguem, J. Eberhardt, SAE Tech. Paper, 1999-01-1512.
[39] G. Knothe, K.R. Steidley, Energy Fuels 19 (2005) 1192.
[40] J. Hu, Z. Du, C. Li, E. Min, Fuel 84 (2005) 1601.
[41] P. Norton, K. Vertin, B. Bailey, N.N. Clark, D.W. Lyons, S. Goguen, J. Eberhardt, SAE Tech. Paper No. 982526, 1998.
[42] K. Nakakita, K. Akihama, W. Weissman, J.T. Farrell, Ind. Eng. Res. 6 (3) (2005) 187.
[43] I.P. Androulakis, M.D. Weeisel, C.S. Hsu, K. Qian, L.A. Green, J.T. Farrell, Energy Fuels 19 (2005) 111.
[44] K. Akihama, Y. Takatori, K. Nakakita, R&D Rev. Toyota 37 (3) (2002) 46.
[45] Y. Takatori, Y. Mandokoro, K. Akihama, K. Nakakita, Y. Tsukasaki, S. Iguchi, L.I. Yeh, A.M. Dean, SAE Tech Paper Ser. No. 982495, 1998.